

Stability and image-potential-induced screening of electron vibrational excitations in a three-layer structure*

G. Meissner, H. Namaizawa,[†] and M. Voss

Theoretische Physik, Universität des Saarlandes, D-66 Saarbrücken, Germany

(Received 5 August 1975)

The relative static stability of square and triangular electron lattices (two-dimensional Wigner crystals), the instability against vibrational excitations, and the effect of image-potential-induced screening on the dispersion of the frequency spectra are studied in the inversion layer of a metal-insulator-semiconductor structure. In harmonic approximation the two-dimensional Wigner crystal turns out to be stable against transverse vibrations for a triangular lattice but unstable for a square lattice in the [10] direction in disagreement with previous calculations. In triangular lattices, the transition of the anomalous dispersion ($\omega_L \propto k^{1/2}$) of the two-dimensional longitudinal mode at intermediate wave vectors ($D^{-1} \ll k \ll a^{-1}$) to the normal dispersion ($\omega_L \propto k$) in the extremely-long-wavelength limit ($kD \ll 1$) due to screening effects is studied as a function of the ratio of insulator thickness D and lattice constant a .

I. INTRODUCTION

Recent measurements of resonance absorption due to transitions between quantized states have verified most directly that electrons can form an essentially two-dimensional system immersed in a uniform background of positive charge either in the surface space-charge layer of a semiconductor¹ or above the surface of liquid helium.² These experiments therefore confirm theoretical predictions³ that at low temperatures a strong electric field in the first case and a combination of an external field and image forces in the second one trap the electrons to their lowest quantum state for motions perpendicular to the surface. As the electron motion parallel to the surface is essentially unrestricted the two-dimensional nature of such systems has also been revealed by electron cyclotron resonance measurements.⁴

All these experiments together raise the possibility to study a variety of further properties of two-dimensional electron systems and theoretical calculations are therefore of great interest. The ratio of mean-kinetic-to-mean-potential energy can for instance be varied over a wide range by experimentally varying the surface concentration of these electrons. Since the kinetic energy of the electrons is small in a dilute system, the question arises whether such systems might exhibit crystallization into a two-dimensional Coulomb solid in order to minimize their potential energy.⁵ Crandall and Williams⁶ first suggested that an ordered state might minimize the potential energy of the electrons above the surface of liquid helium by forming a two-dimensional Wigner crystal. Independently, Chaplik⁷ discussed the possibility of crystallization of charge carriers in low-density inversion layers and investigated qualitatively the long-wavelength limit of vibrational excitations.

In particular, the anomalous dispersion, $\omega_L \propto k^{1/2}$, of the longitudinal plasmonlike acoustic branch at long wavelength ($k \ll a^{-1}$), in addition to a transverse branch, $\omega_T \propto k$, has first been predicted in Ref. 7. The experimental possibility of a liquid-solid transition has been concluded by Platzman and Fukuyama⁸ based on the study of the phase diagram of such two-dimensional electron systems. A λ -type transition between a fluid and a poly-microcrystalline phase has been discovered by Hockney and Brown⁹ in a system of classical point charges confined to move in a plane using a molecular-dynamics method. Experimental evidence, however, concerning the existence of crystallization of electrons in the lowest quantum state at a surface is still inconclusive at present.

The dynamical stability of two-dimensional electron lattice structures and possible effects on the frequency spectra associated with the experimentally given three-layer structure, e.g., metal-insulator-semiconductor, are interesting from a theoretical and experimental point of view. Therefore, the main object of the present paper is to investigate quantitatively two-dimensional Wigner lattices, in particular, with respect to the stability against vibrational excitations taking into account image-potential-induced screening effects due to a three-layer structure for various thicknesses D of the intermediate insulator.

The underlying model of a three-layer structure is outlined in Sec. II. The general approach for investigating vibrational excitations of electron lattices is set up in Sec. III. As an application we find, for instance, that in the harmonic approximation the frequencies of transverse vibrations of a square lattice are imaginary around the [10] direction, in disagreement with previous calculations.¹⁰ Whereas, in a triangular lattice the frequencies of both modes in the plane are real every-

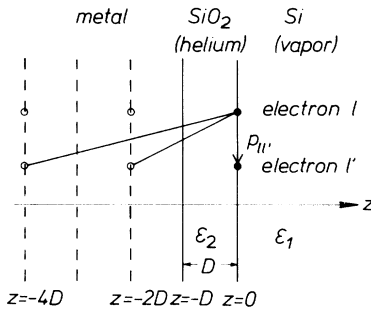


FIG. 1. Interaction of two electrons of distance $\rho_{1l'}$ at the interface $z=0$ in a three-layer structure, e.g., semiconductor (Si)-insulator (SiO_2)-metal, or equivalently, vapor-helium metal. The induced image charges are located on planes $z=-2D, -4D, \dots$.

where in the Brillouin zone. We conclude that a triangular structure is stable but a square structure is unstable against external shearing forces corresponding to wave propagation around the [10] direction. Based on this fact we restrict our detailed calculations to a triangular structure. In Sec. IV image-potential-induced screening effects on the electron vibrational excitations are investigated quantitatively as a function of the insulator thickness D in a three-layer structure. Implications of our work on experimentally observing a two-dimensional Wigner lattice are briefly indicated in the conclusions of Sec. V.

II. MODEL OF THREE-LAYER STRUCTURE

A schematic view of our three-layer system is given in Fig. 1. The semiconductor (Si with dielectric constant $\epsilon_1 \approx 11.8$) is filling the space $z > 0$, the insulating layer (SiO_2 with dielectric constant $\epsilon_2 \approx 3.8$) the space between $z=0$ and $z=-D$, and the metal the space $z < -D$. We assume that at low temperatures all the electrons in the inversion layer are in their lowest quantum state with respect to motion in z direction and, for simplicity, set the expectation value of z in this state equal to zero, i.e., we assume all the electrons to be situated at the interface between the semiconductor and the insulator. The electrostatic interaction energy between two electrons (charge e) of distance $\rho_{1l'}$, $= |\vec{x}_l - \vec{x}_{l'}|$ at the interface $z=0$ then reads

$$W(\rho_{1l'}) = \frac{e^2}{\bar{\epsilon}} \left(\frac{1}{\rho_{1l'}} - \frac{\epsilon_2}{\bar{\epsilon}} \sum_{\nu=1}^{\infty} K^{\nu-1} \frac{1}{[\rho_{1l'}^2 + (2\nu D)^2]^{1/2}} \right), \quad (1)$$

where $\bar{\epsilon} \equiv \frac{1}{2}(\epsilon_1 + \epsilon_2)$ and $K \equiv (\epsilon_1 - \epsilon_2)/(\epsilon_1 + \epsilon_2)$. The first term in (1) denotes the direct Coulomb repulsion between the electrons of "renormalized" charges $e/\bar{\epsilon}^{1/2}$ and the following sum denotes the attractive interaction induced by an infinite series of positive image charges located in the metal on

the planes $z = -2D, -4D, \dots, -2\nu D, \dots$. The relative strength of the ν th image charge is determined by $K^{\nu-1}$. Therefore, $W(\rho_{1l'})/e$ corresponds to the potential $\Phi(\rho_{1l'}, z_l = z_{l'} = 0)$, induced by a charge e at a distance $\rho_{1l'}$ in region $z > 0$ of the system, satisfying Poisson's equation with appropriate boundary conditions at the interfaces.

From Eq. (1) we may readily obtain two limiting cases.⁷ For thick insulating layers, $D \gg \rho_{1l'}$, the Coulomb repulsion between renormalized charges dominates, i.e., $W(\rho_{1l'}) \approx e^2/(\rho_{1l'} \bar{\epsilon})$. In the opposite limit of thin insulating layers, $\rho_{1l'} \gg D$, however, the image charges cancel the direct Coulomb term, since electrons and image charges are approximately forming dipoles and the effective interaction becomes

$$W(\rho_{1l'}) \approx 2\epsilon_1 \frac{D^2}{\epsilon_2^2} \frac{e^2}{\rho_{1l'}^3}.$$

The additional attractive field induced by the image charges of a three-layer structure thus gives rise to a screening of the bare Coulomb repulsion of the electrons in the surface layer. The Fourier transform of $W(\rho_{1l'})$ with respect to the two-dimensional vector $\rho_{1l'}$ can be written

$$\begin{aligned} W(|\vec{k}|) &\equiv \int_0^{\infty} d\rho \rho W(\rho) \int_0^{2\pi} d\phi e^{-i\vec{k} \cdot \vec{\rho}} \\ &= \frac{1}{\bar{\epsilon}} \frac{2\pi e^2}{|\vec{k}|} \frac{1 - e^{-2kD}}{1 - Ke^{-2kD}}, \end{aligned} \quad (2)$$

showing explicitly that the electrostatic interaction energy of Eq. (1) corresponds to the form actually used by Chaplik.⁷ Our numerical investigations are based on Eq. (1). They reveal, e.g., a dynamical instability of the square lattice. Therefore, we conclude that the matrix of the elastic constants for a square lattice calculated by Chaplik⁷ must contain negative principal minors giving rise to unphysical imaginary sound velocities for certain directions and polarizations.

From Eq. (2) we find that $W(|\vec{k}|)$ remains finite at $k=0$ for noninfinite values of the layer thickness ($D < \infty$), i.e., $W(\vec{k}=0) = 2\pi e^2 2D/\epsilon_2$. Only in the limit $D \rightarrow \infty$ we obtain $W(\vec{k}) = (2\pi e^2/\bar{\epsilon})/|\vec{k}|$ which corresponds to the Fourier transform of the bare Coulomb interaction in two dimensions and thus diverges at $k=0$ due to the infinite range of the interaction.

III. FORMAL DEVELOPMENT

In this section we review the formal basis of a theory¹¹ appropriate for a study of vibrational properties of two-dimensional electron lattices along with their static stability and possible dynamical instabilities. Our model Hamiltonian is given by

$$H = T_e + T_i + V,$$

with the kinetic energies of electrons T_e and neutralizing "ion" charges T_i , respectively. The potential energy

$$V = V_{e-e} + V_{e-i} + V_{i-i}$$

contains the electron-electron interaction V_{e-e} , the interaction of the electrons with the uniform background of ions V_{e-i} , and the interaction of the background ions V_{i-i} . In order to account for the modification of the Coulomb interaction by the presence of the insulator and the metallic gate electrode we are using the screened potential $W(\vec{x}_i - \vec{x}_{i'})$ of (1) instead of $e^2/|\vec{x}_i - \vec{x}_{i'}|$, i. e.,

$$V_{e-e} = \frac{1}{2} \sum_{i \neq i'} W(\vec{x}_i - \vec{x}_{i'}) \quad (3)$$

and

$$V_{e-i} + V_{i-i} = - \sum_i \frac{N}{F} \int d^2\rho W(\vec{x}_i - \vec{\rho}) + \frac{1}{2} \left(\frac{N}{F}\right)^2 \int d^2\rho \int d^2\rho' W(\vec{\rho} - \vec{\rho}') . \quad (4)$$

The electron density per unit area, $N/F \equiv n = 1/(\pi r_s^* a_0^2)$, is measured in terms of the dimensionless mean interparticle separation r_s^* , where $a_0 = \hbar^2/me^2$ denotes the three-dimensional Bohr radius.

A certain lattice structure will be defined by identifying the equilibrium positions $\langle x_{\alpha}(l) \rangle$ of electrons with the lattice sites of a two-dimensional lattice. For Bravais lattices thus

$$\langle x_{\alpha}(l) \rangle \equiv R_{\alpha}(l) = A_{\alpha\alpha'} l_{\alpha'} ,$$

where $\alpha, \alpha' = 1, 2$ and $l_{\alpha'} = 0, \pm 1, \pm 2, \dots$. Finally, $A_{\alpha\alpha'}$ denotes the two-by-two matrix of the unit cell. The area of the unit cell $F_0 = \det \mathbf{A}$ and the electron density per unit area $n = 1/F_0$.

Before discussing the dynamical behavior of two-dimensional electron lattices it is worth investigating some static features. In this context the mean static energy $\langle V \rangle/N$ provides a first indication of the relative stability of a given lattice structure. In a harmonic treatment of our dilute electron system, e. g., we may approximate the averages of the interaction energies $\langle W \rangle$ in (3) and (4) by replacing all instantaneous electron positions \vec{x} by their mean values, for instance, $\langle W(\vec{x}_i - \vec{x}_{i'}) \rangle \approx W(\langle \vec{x}(l) \rangle - \langle \vec{x}(l') \rangle)$. Therefore, in harmonic approximation

$$\frac{\langle V \rangle}{N} \approx \frac{1}{2} \sum_{i \neq i'} W(\vec{R}(l)) - \frac{1}{2} n \int d^2\rho W(\vec{\rho}) . \quad (5)$$

Results of a numerical evaluation of (5) will be presented in Sec. IV.

For explicitly calculating vibrational frequencies of the Coulomb solid it is important to note that in two dimensions—differently from three

dimensions¹²—only the electron-electron interaction V_{e-e} , i. e., Eq. (3), of the Hamiltonian H enters into the expressions for the electron vibrational excitations. This can be shown quite generally by employing sum-rule arguments¹³ in evaluating the rigorous expression of the self-energy of vibrational excitations¹¹:

$$M(12) = \delta \left\langle \frac{\partial H}{\partial x(1)} \right\rangle / \delta \langle x(2) \rangle , \quad (6)$$

where $x(1)$ denotes the Cartesian component α_1 of the position operator of the electron l_1 at time t_1 , i. e., $1 \equiv \alpha_1 l_1 t_1$. Since we are interested in properties of a dilute electron system we may investigate the self-energy of (6) in harmonic approximation (HA), where

$$M(12) \approx \delta(t_1 - t_2) \Phi_{\alpha_1 \alpha_2}(l_1 l_2) . \quad (6a)$$

The two eigenvalues of the Fourier transform $\Phi_{\alpha_1 \alpha_2}(\vec{k})$ of the force-constant tensor $\Phi_{\alpha_1 \alpha_2}(l_1 l_2)$ give then the squared vibrational frequencies of the electron lattice in the interface plane in HA:

$$\omega_{\pm}^2(\vec{k}) = \frac{1}{2} (\tilde{\Phi}_{11}(\vec{k}) + \tilde{\Phi}_{22}(\vec{k}) \pm \{[\tilde{\Phi}_{11}(\vec{k}) - \tilde{\Phi}_{22}(\vec{k})]^2 + 4\tilde{\Phi}_{12}^2(\vec{k})\}^{1/2}) . \quad (7)$$

With Eq. (1) for W , and appropriately chosen dimensionless variables, one finds

$$\tilde{\Phi}_{\alpha_1 \alpha_2}(\vec{k}) = \omega_0^2 \left(\Phi_{\alpha_1 \alpha_2}^*(\vec{k}^*; 0) - \frac{\epsilon_2}{\epsilon} \sum_{\nu=1} K^{\nu-1} \Phi_{\alpha_1 \alpha_2}^*(\vec{k}^*; \zeta_{\nu}^*) \right) , \quad (8)$$

where $\vec{k}^* \equiv (a/2\pi)\vec{k}$, $\zeta_{\nu}^* \equiv 2\nu D/a$, and

$$\Phi_{\alpha_1 \alpha_2}^*(\vec{k}^*; \zeta_{\nu}^*) = \sum_{\vec{R}^*(l) \neq 0} [1 - e^{2\pi i \vec{k}^* \cdot \vec{R}^*(l)}] \times \nabla_{\alpha_1}^* \nabla_{\alpha_2}^* \frac{1}{[R^{*2}(l) + \zeta_{\nu}^{*2}]^{1/2}} . \quad (9)$$

The frequency $\omega_0 \equiv (e^2/(\bar{\epsilon} m a^3))^{1/2}$ and the lattice sites in units of lattice spacing a are $R_{\alpha}^*(l) \equiv a^{-1} R_{\alpha}(l)$. A quantitative evaluation of the vibrational excitations of a triangular lattice based on Eq. (7) will be presented in Sec. IV.

Taking into account the oscillations of the electrons about their lattice sites we obtain the internal energy $\langle H \rangle/N$ in HA by adding the vibrational energy

$$E_{\text{vib}} \approx N^{-1} \sum_{kj} \hbar \omega_j(\vec{k}) [n(\hbar \omega_j(\vec{k})) + \frac{1}{2}]$$

to the static energy of Eq. (5), where the polarization index $j = \pm$ and the Bose distribution function $n(\hbar \omega) = (e^{\hbar \omega/k_B T} - 1)^{-1}$. At sufficiently low temperatures T where $n(\hbar \omega) \rightarrow 0$ the internal energy is obtained by adding to the static energy the zero-point energy

$$E_0 = N^{-1} \sum_{\vec{k}, j} \frac{1}{2} \hbar \omega_j(\vec{k})$$

to be calculated via a summation of the vibrational frequencies $\omega_j(\vec{k})$ over the two-dimensional Brillouin zone. Therefore, in HA as $T \rightarrow 0$

$$\begin{aligned} \frac{\langle H \rangle}{N} &\simeq \frac{1}{2} \sum_{\vec{l} \neq 0} w(\vec{R}(\vec{l})) - \frac{1}{2} n \int d^2 \rho W(\vec{\rho}) \\ &+ N^{-1} \sum_{\vec{k}, j} \frac{1}{2} \hbar \omega_j(\vec{k}). \end{aligned} \quad (10)$$

In using dimensionless variables $\vec{R}^* \equiv a^{-1} \vec{R}$ and $\omega_j^* \equiv \omega_j^{-1} \omega_j$ in (10) we readily find that the static-energy term $\langle V \rangle / N \propto -1/r_s^*$ and that the zero-point energy term $E_0 \propto 1/r_s^{*3/2}$. The results of evaluating the numerical constant in front of $1/r_s^{*3/2}$ will also be presented in Sec. IV.

IV. PRESENTATION OF RESULTS FOR SCREENED TWO-DIMENSIONAL ELECTRON LATTICES

The numerical evaluation of the mean static energy $\langle V \rangle / N$ of Eq. (5), of the two vibrational frequencies $\omega_{\pm}(\vec{k})$ of Eq. (7) by means of Eqs. (8) and (9), and of the zero-point energy term in Eq. (10) has been carried out by a computer. The lattice sums required for evaluating Eq. (5) and Eq. (9) are converging rather slowly. We, therefore, have applied the Ewald method¹⁴ in order to perform the lattice summations. The summation of the frequencies $\omega_j(\vec{k})$ over the two-dimensional Brillouin zone in the zero-point energy term of Eq. (10) has been performed by appropriately averaging over a coarse mesh of 256 different \vec{k} vectors distributed uniformly over the first Brillouin zone of the triangular lattice with an irreducible segment of $\frac{1}{12}$.

A. Relative static stability

The matrices of the unit cell for the triangular lattice and the square lattice are

$$(A_{\alpha\alpha'}) = a \begin{pmatrix} 1 & \frac{1}{2} \\ \frac{1}{2} & \sqrt{3} \end{pmatrix} \quad \text{and} \quad (A_{\alpha\alpha'}) = a \begin{pmatrix} 1 & 0 \\ 0 & 1 \end{pmatrix},$$

respectively. In calculating the mean static energies $\langle V \rangle / N$ of these "ideal" two-dimensional systems ($D \rightarrow \infty$ and $\bar{\epsilon} = 1$) from Eq. (5) in units of Ry $\equiv e^2 / 2a_0$ we find a value of $-2.21/r_s^*$ Ry for the triangular lattice and a value of $-2.20/r_s^*$ Ry for the square lattice, i. e., the triangular lattice is the configuration of lowest potential energy.¹⁵

B. Dynamical instability and dispersion curves

However, in addition to the relative static stability of a triangular lattice as compared with a square lattice, our numerical calculations reveal an *instability* of the square lattice against transverse vibrational excitations in harmonic approximation. The frequency squares of the transverse branch

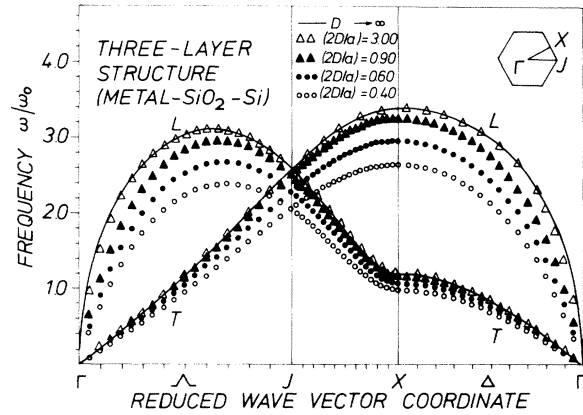


FIG. 2. Dispersion curves for a triangular electron lattice in a three-layer system along the Λ direction and the Δ direction and the connecting line on the zone surface at various reduced insulator thicknesses $2D/a$.

of vibrational excitations in the $[10]$ direction of a square lattice are given by the diagonal component $\bar{\Phi}_{22}(\vec{k})$ of Eq. (8) with $\vec{k} \parallel [10]$. Numerically we obtain $\bar{\Phi}_{22}(\vec{k}) < 0$ for $\vec{k} \parallel [10]$. The transverse branch in $[10]$ direction therefore turns out to be imaginary in contrast to previous calculations.¹⁰ This behavior holds even more generally for the frequencies $\omega_{\pm}(\vec{k})$ of wave vectors \vec{k} around the $[10]$ direction. It is because of this dynamical instability of the square lattice against shear forces that we present dispersion curves of the triangular lattice configuration exclusively.

For a quantitative investigation of the screening effects on the frequency spectra as a function of the ratio of insulator thickness D and lattice particle separation a we have computed from Eq. (7) the dispersion curves in the main symmetry directions and their connections along the zone boundary of a triangular lattice. These dispersion curves $\omega_{\pm}(\vec{k})$ are plotted in Fig. 2 in units of ω_0 defined above where the mass m should denote the effective electron mass of the planar motion parallel to the interface. The solid lines represent the dispersion curves for the limiting case ($D \rightarrow \infty$) where two half-spaces are filled by SiO_2 and Si , respectively. In this limit one obtains the electron vibrational spectra of the "ideal" two-dimensional Wigner crystal for $\bar{\epsilon} = 1$.¹⁶ The solid lines of the longitudinal modes clearly show the two-dimensional plasma dispersion behavior,¹⁷ $\omega_L(\vec{k}) \propto k^{1/2}$, at small wave vectors k . The four transverse and longitudinal curves appearing in addition in Fig. 2 correspond to values of 0.40, 0.60, 0.90, and 3.00 for $2D/a$, where twenty image charges have been included according to Eq. (8). The curves for the value 3.00 are already quite close to the dispersion curves for the ideal case ($D \rightarrow \infty$). A transition from the anomalous

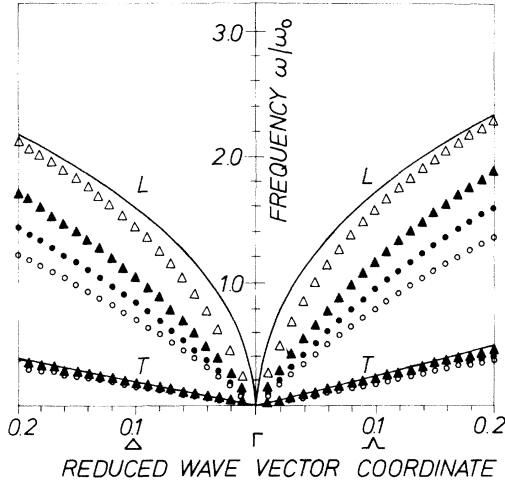


FIG. 3. Dispersion curves of the vibrational excitations of a triangular electron lattice in the vicinity of the Γ point along the Δ direction and the Λ direction.

dispersion $\omega_L \propto k^{1/2}$ to a linear dispersion $\omega_L = s_L k$ at sufficiently small k with decreasing $2D/a$ is rather clearly seen in Fig. 3 where the dispersion curves are drawn on an enlarged scale in the vi-

cinity of the Γ point along the Λ line and the Δ line, respectively. The transverse branches, on the other hand, are linear in k for $k \rightarrow 0$ also in the "ideal" case and their "sound" velocities s_T —to be obtained from the slope of the dispersion curves—do not change so much with the thickness D of the insulating layer. The dependence of ω_L^*/k^* on the reduced insulator thickness $2D/a$ is plotted in Fig. 4 for wave propagation along the Δ line. The four points of this plot correspond to the smallest \vec{k} -vector points of Fig. 3 where the linear dispersion $\omega_L = s_L k$ should already be valid approximately. From the slope of a fit of these points by a straight line (dotted line) we may infer a square-root dependence $s_L \propto (2D/a)^{1/2}$.

The transition of the dispersion relation of longitudinal electron vibrations in a three-layer structure from a two-dimensional plasmon dispersion to a linear one in the extreme long-wavelength limit, the square-root dependence of the longitudinal sound velocity on the reduced insulator thickness, and the linear wave-vector dependence of the transverse excitation frequencies are rather general phenomena which hold independently from the details of the structure. Qualitatively these results may readily be obtained by rewriting Eq. (8) in a series in reciprocal-lattice space^{7,11}:

$$\begin{aligned} \bar{\Phi}_{\alpha_1 \alpha_2}(\vec{k}) = & (2\pi\omega_0)^2 n a^2 \left[\frac{\vec{k}_{\alpha_1}^* \vec{k}_{\alpha_2}^*}{|\vec{k}^*|} \frac{1 - \exp(-2\pi k^* \zeta_1^*)}{1 - K \exp(-2\pi k^* \zeta_1^*)} + \sum_{\vec{G}^* \neq 0} \left(\frac{(\vec{G}^* + \vec{k}^*)_{\alpha_1} (\vec{G}^* + \vec{k}^*)_{\alpha_2}}{|\vec{G}^* + \vec{k}^*|} \frac{1 - \exp(-2\pi |\vec{G}^* + \vec{k}^*| \zeta_1^*)}{1 - K \exp(-2\pi |\vec{G}^* + \vec{k}^*| \zeta_1^*)} \right. \right. \\ & \left. \left. - \frac{\vec{G}_{\alpha_1}^* \vec{G}_{\alpha_2}^*}{|\vec{G}^*|} \frac{1 - \exp(-2\pi |\vec{G}^*| \zeta_1^*)}{1 - K \exp(-2\pi |\vec{G}^*| \zeta_1^*)} \right) \right], \end{aligned} \quad (11)$$

with the reduced reciprocal lattice vectors $\vec{G}^* \equiv (a/2\pi)\vec{G}$ given, e.g., through the Cartesian components $G_{\alpha'} = 2\pi h_{\alpha'} B_{\alpha\alpha'}$, where $h_{\alpha'} = 0, \pm 1, \pm 2, \dots$. In a triangular lattice

$$(B_{\alpha\alpha'}) = a^{-1} \begin{pmatrix} 1 & -1/\sqrt{3} \\ 0 & 2/\sqrt{3} \end{pmatrix}.$$

Neglecting for $k \ll a^{-1}$ the sum over all terms $\vec{G}^* \neq 0$ in (11) one obtains for the longitudinal vibrational frequency

$$\omega_L(\vec{k}) \simeq 2\pi\omega_0 \left(n a^2 k^* \frac{1 - \exp(-2\pi k^* \zeta_1^*)}{1 - K \exp(-2\pi k^* \zeta_1^*)} \right)^{1/2}. \quad (12)$$

The anomalous dispersion following from (12) in the region $D^{-1} \ll k \ll a^{-1}$,

$$\omega_L(\vec{k}) = 2\pi\omega_0 (n a^2)^{1/2} k^{*1/2}, \quad (12a)$$

then corresponds to the dispersion relation of two-dimensional plasmons. For $D \rightarrow \infty$ the dispersion relation (12a) holds down to $k = 0$ owing to the long-range Coulomb interaction. For $D < \infty$, however,

the screening induced by the image charges reduces this anomalous dispersion to a normal, i.e., a linear dispersion at still smaller wave vectors $kD \ll 1$:

$$\omega_L(\vec{k}) = 2\pi\omega_0 [n a^2 (\bar{\epsilon}/\epsilon_2) 2\pi \zeta_1^*]^{1/2} k^*. \quad (12b)$$

Since the contribution from the reciprocal-lattice vectors $\vec{G}^* \neq 0$ is irrelevant for this transition it is clear that this behavior remains essentially valid for the plasma modes of a two-dimensional *electron gas* in the inversion layer of a metal-insulator-semiconductor structure.¹⁸ The square-root dependence of ω_L^*/k^* on $\zeta_1^* \equiv 2D/a$ following from (12b) has been drawn in Fig. 4 (solid line).

Disregarding umklapp processes, i.e., terms $\vec{G}^* \neq 0$ in (11), one obtains $\omega_T(\vec{k}) \equiv 0$ due to the resulting vanishing transverse sound velocities and the vanishing shear moduli. This result, of course, is associated with the fact that umklapp vibrational excitations are related to Goldstone excitations of broken translational invariance¹⁹ and thus responsible for nonvanishing shear moduli and nonvanishing transverse sound velocities in

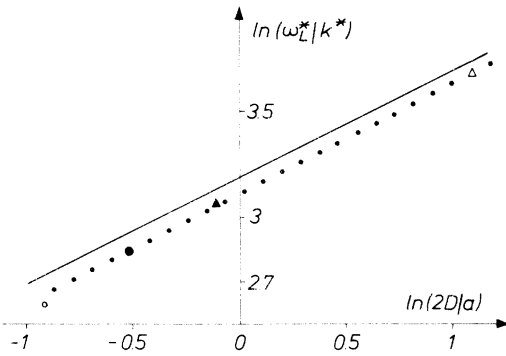


FIG. 4. Logarithmic plot of the ratio ω_L^*/k^* vs the reduced insulator thickness $2D/a$ for wave propagation along the Δ line. The solid line follows from Eq. (12b); the dotted line represents the fit of ω_L^*/k^* for four values $2D/a$ at $\frac{1}{100}$ of the maximum wave vector of the first Brillouin zone.

the solid phase. The large wave vectors, $\vec{G}^* \neq 0$, on the other hand, are not essentially affected by screening effects as caused by small values $2D/a$. This observation is in accord with our numerical results that the linear dispersion of transverse vibrations in the long-wavelength limit holds irrespectively of the insulator thickness and that the transverse sound velocities do not change drastically with the thickness of the insulating layer.

Finally, it should be noted that the transverse dispersion curves in Fig. 2 exhibit a small upward curvature in the middle of the first Brillouin zone along the Λ line. The anomalous positive dispersion is most clearly seen in the limit of the ideal two-dimensional Wigner crystal and becomes less evident for decreasing values of the insulator thickness D . From the graphical representation we may conjecture that this anomalous curvature of the dispersion is a result of long-range interaction since in the ideal case the transverse dispersion in the long-wavelength limit in the Λ direction has to remain linear; yet it still must match the continuation of the longitudinal dispersion along the Δ line with the anomalous square-root behavior at the Γ point due to the long-range Coulomb forces.

C. Zero-point energy

Having calculated the normal-mode frequencies of the electron vibrational excitations at sufficient \vec{k} vectors in the first Brillouin zone one obtains the zero-point energy E_0 by numerical integration. We find a value of $1.63/\gamma_s^{*3/2}$ Ry for the ideal triangular lattice. The prefactor in front of $1/\gamma_s^{*3/2}$ decreases with decreasing insulator thickness D .

V. CONCLUSIONS

The present investigations have explicitly been concerned with the study of the influence of a three-layer structure on the vibrational excitations of

charge-compensated electrons in a planar geometry with their Coulomb interaction predominating. From our numerical calculations as well as the general arguments it is clear that the longitudinal vibrations of such a two-dimensional Wigner crystal in the long-wavelength limit qualitatively exhibit the same form as an electron gas. Though the present calculations in harmonic approximation could be used generally for analyzing measurements of two-dimensional vibrational excitations in this regime, which are still lacking yet, only transverse vibrations would, of course, give experimental evidence of crystallization of electrons.

The present approach¹¹ outlined in Sec. III, however, by no means is limited to the harmonic approximation (HA) which should rather be considered as a first application. A straightforward extension of the HA to the renormalized harmonic approximation (RHA), consists in calculating mean values of interaction energies of the form $\langle W(\vec{x}_l, -\vec{x}_{l'}) \rangle$ by weighting deviations from equilibrium distances between two electrons at l and l' with a Gaussian having a width which is determined by the equal-time relative displacement correlation function (RDCF). Owing to the resulting functional dependence of the effective force-constant tensor on the RDCF in the RHA a sum rule for the kinetic energy²⁰ imposes a self-consistency condition on the RDCF giving rise to the possibility of describing a first-order phase transition. Kugler²¹ has actually suggested to apply the RHA in order to study the stability of a three-dimensional Wigner crystal, and Fukuyama and Platzman⁸ have elaborated the theory further with respect to the possible crystallization into a two-dimensional Coulomb solid. In that connection it is important to note that the RDCF, entering into the effective force constants in RHA does not diverge in two dimensions in contrast to the autocorrelation function of displacements.^{22,23} For these reasons the RHA can even be applied to the problem of an "isolated" two-dimensional Wigner crystal.²⁴

However, in the planar geometry of a charge-compensated electron system considered in this paper the degree of freedom of the total momentum corresponding to translations perpendicular to the interface should not be neglected from the beginning. In the language of broken translational invariance a second transverse vibrational mode follows from that degree of freedom describing a drumlike vibration (polarization perpendicular to the interface) in addition to the transverse vibrational mode of polarization parallel to the interface investigated above. Associated with the drumlike transverse mode, finally, is another instability which should set in with increasing surface concentration of electrons deserving, however, a separate detailed analysis.

- *A short account of this work was reported at the Spring Meeting of the "Deutsche Physikalische Gesellschaft", Münster, Germany, March 17-22, 1975 by G. Meissner, H. Namaizawa and M. Voss, *Verhandl. DPG (VI)* **10**, 647 (1975).
- †On leave of absence from Institute of Physics, College of General Education, University of Tokyo, Komaba 3-8-1, Tokyo, Japan.
- ¹A. Kamgar, P. Kneschaurek, G. Dorda, J. F. Koch, *Phys. Rev. Lett.* **32**, 1251 (1974).
- ²C. C. Grimes and T. R. Brown, *Phys. Rev. Lett.* **32**, 280 (1974).
- ³W. M. Cole and M. H. Cohen, *Phys. Rev. Lett.* **23**, 1238 (1969); V. B. Shikin, *Zh. Eksp. Teor. Fiz.* **58**, 1748 (1970) [*Sov. Phys. -JETP* **31**, 936 (1970)]; F. Stern and W. E. Howard, *Phys. Rev.* **163**, 816 (1967).
- ⁴T. R. Brown and C. C. Grimes, *Phys. Rev. Lett.* **29**, 1233 (1972); G. Abstreiter, P. Kneschaurek, J. P. Kotthaus, and J. F. Koch, *ibid.* **32**, 104 (1974); B. J. Allen, Jr., D. C. Tsui, and J. V. Dalton, *ibid.* **32**, 107 (1974).
- ⁵The suggestion of crystallization into a three-dimensional Coulomb solid dates back to E. P. Wigner, *Phys. Rev.* **46**, 1002 (1934); *Trans. Faraday Soc.* **34**, 678 (1938).
- ⁶R. S. Crandall and R. Williams, *Phys. Lett. A* **34**, 404 (1971).
- ⁷A. V. Chaplik, *Zh. Eksp. Teor. Fiz.* **62**, 746 (1972) [*Sov. Phys. -JETP* **35**, 395 (1972)].
- ⁸P. M. Platzman and H. Fukuyama, *Phys. Rev. B* **10**, 3150 (1974).
- ⁹R. W. Hockney and T. R. Brown, *J. Phys. C* **8**, 1813 (1975).
- ¹⁰R. S. Crandall, *Phys. Rev. A* **8**, 2136 (1973).
- ¹¹G. Meissner, *Festkörperprobleme XIII (Advances in Solid State Physics)*, edited by H. J. Queisser (Pergamon-Vieweg, Braunschweig, 1973), p. 359.
- ¹²See, e.g., R. A. Coldwell-Horsfall, and A. A. Maradudin, *J. Math. Phys.* **1**, 395 (1960).
- ¹³G. Meissner, *Verhandl. DPG (VI)*, **10**, 646 (1975).
- ¹⁴J. M. Ziman, *Principles of the Theory of Solids* (Cambridge U.P., Cambridge, 1964).
- ¹⁵A calculation of the mean static energy for a three-layer structure ($D < \infty$) using Eq. (4) or Eq. (5), respectively, rests on the *ad hoc* assumption that the image-potential-induced screening of the electron-ion and ion-ion interaction is of the same form as the one derived for the electron-electron interaction according to Eq. (1). Such calculations would therefore be more limited than calculations of the dependence of the electron vibrational frequencies on the relative insulator thickness $2D/a$ since they depend on the electron-electron interaction only as shown in Ref. 13.
- ¹⁶The vibrational frequency spectra of our work in the limit $D \rightarrow \infty$ and $\epsilon = 1$ should be directly comparable with those computed by Platzman and Fukuyama, Ref. 8. Since we, however, find, e.g., a reciprocal-lattice spacing $2/\sqrt{3}$ times that stated in Ref. 8, a different orientation of the Brillouin zone, etc., such a comparison is actually not possible.
- ¹⁷See, for instance, H. Kanazawa, *Prog. Theor. Phys.* **26**, 851 (1961).
- ¹⁸This effect of a three-layer structure on the long-wavelength longitudinal plasma modes of an inversion-layer electron gas has been investigated independently by A. Equilez, T. K. Lee, J. J. Quinn, and K. W. Chui (*Phys. Rev. B* **11**, 4989 (1975) with essentially similar results.
- ¹⁹G. Meissner, *Z. Phys.* **205**, 249 (1967).
- ²⁰See, for instance, G. Meissner, *J. Phys. Soc. Jpn. Suppl.* **12**, 143 (1970).
- ²¹A. Kugler, *Ann. Phys. (N.Y.)* **53**, 138 (1969).
- ²²G. Meissner, *Phys. Rev. B* **1**, 1822 (1970).
- ²³D. Mermin, *Phys. Rev.* **176**, 250 (1968).
- ²⁴The problem of stability of a two-dimensional solid without truly long-range positional order has further been investigated by J. M. Kosterlitz and D. J. Thouless, *J. Phys. C* **6**, 1181 (1973).